

DIFFERENTIAL MEASUREMENT OF COSMIC-RAY GRADIENT WITH RESPECT TO INTERPLANETARY CURRENT SHEET

S. P. Christon, A. C. Cummings, and E. C. Stone
California Institute of Technology

K. W. Behannon, and L. F. Burlaga
Goddard Space Flight Center

ABSTRACT

Simultaneous magnetic field and charged particle measurements from the Voyager spacecraft at heliographic latitude separations from 10° to 21° are used to determine the latitude gradient of the galactic cosmic ray flux with respect to the interplanetary current sheet. By comparing the ratio of cosmic ray flux at Voyager 1 to that at Voyager 2 during periods when both spacecraft are first north and then south of the interplanetary current sheet, we find an estimate of the latitudinal gradient with respect to the current sheet of approximately -0.15 ± 0.05 %/deg under restricted interplanetary conditions.

1. Introduction. Organization of cosmic ray flux about the heliographic equator should result from symmetries in the interplanetary magnetic field produced by the sun's rotation. However, if particle drifts are important in cosmic ray transport, the cosmic ray flux should be organized with respect to the interplanetary current sheet. This symmetrizing property of the current sheet has been demonstrated in a three-dimensional model of cosmic ray transport including particle drifts [Kota and Jokipii, 1983]. At 1 AU, gradients with respect to the current sheet G_θ of up to ~ -0.33 %/deg have been identified for cosmic ray protons with energies >100 MeV in various integral energy ranges [Newkirk et al., 1984; Newkirk and Fisk, 1985].

The interplanetary current sheet is a surface separating regions of magnetic field pointing generally toward or away from the sun. In its least complicated configuration, the near-sun current sheet is essentially a circle tilted with respect to the heliographic equator. As the rotating sun's magnetic field is drawn out by the solar wind, warping of the current sheet ensues, thus allowing two spacecraft separated in latitude to sample fluxes on either side of it (Figure 1). The near-sun current sheet extends up to $\sim 60^\circ$ north and south S of the equator and produces an interplanetary sector pattern that varies between two and four sectors during the period of this study [Hoeksema, 1984].

We determine G_θ using spacecraft trajectory information, the ratio of cosmic ray flux, and observations of the current sheet (magnetic field sector boundaries) at Voyager 1 (V1) and Voyager 2 (V2), separated in latitude by 10° to 21° . Such a differential measurement has significantly smaller non-latitudinal intensity variations than a single-point measurement such as the type employed by Newkirk et al. and Newkirk and Fisk. The cosmic ray flux at an observation point in the heliosphere is $j = j_b \exp(G_r(r-R_b)) \exp(G_\theta(\theta-\theta_{cs}))$, where G_r is the radial gradient, G_θ is the colatitude gradient with respect to the current sheet, R_b is the radius of the boundary of the heliosphere, j_b is the cosmic ray flux at R_b , assumed constant, θ_{cs} is the colatitude of the current sheet, and r and θ are the radius and colatitude of the observation point. Heliographic colatitudes θ from 0° to 180° correspond to

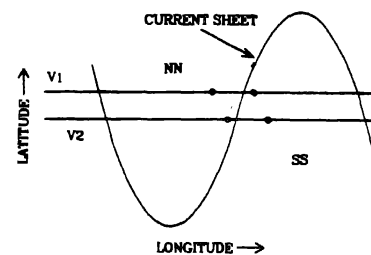


Fig. 1. Schematic representation of NN and SS configuration.

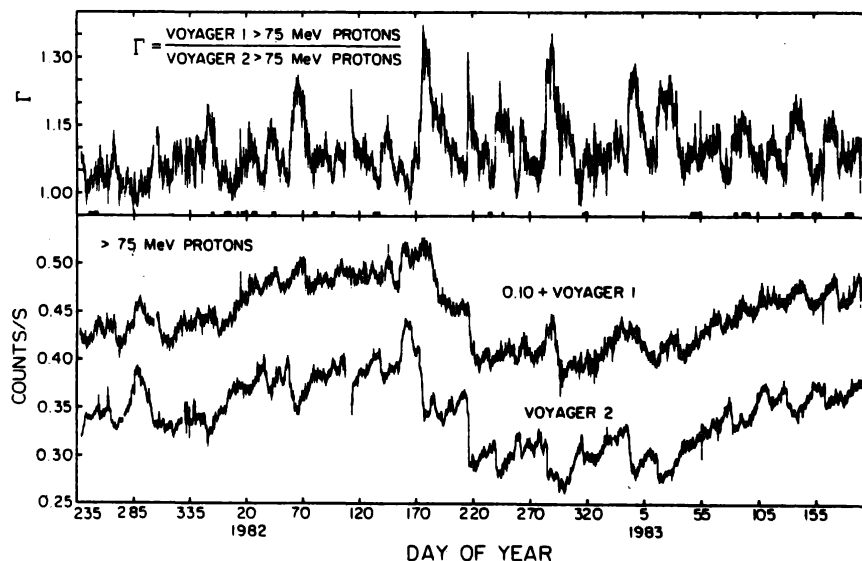
heliographic latitudes from 90°N to 90°S. Time series of simultaneous observations at two points in interplanetary space well separated in latitude allow estimates of G_θ to be obtained for each interval in the series. These individual estimates of $G_\theta = (\ln \Gamma - G_r (\tau_1 - \tau_2)) / (\theta_1 - \theta_2)$, where the subscripts 1 and 2 refer to V1 and V2, respectively, and Γ is the ratio of the flux at V1 to that at V2, are independent of variations in the separation of the observation points. Statistically weighted averages of

$\langle G_\theta \rangle_{NN(SS)} = \sum_{i(j)} w_{\theta i(j)} G_{\theta i(j)} / \sum_{i(j)} w_{\theta i(j)}$ and $\langle G_r \rangle = \left(\sum_i w_{\theta i} G_{\theta i} - \sum_j w_{\theta j} G_{\theta j} \right) / \left(\sum_i w_{\theta i} + \sum_j w_{\theta j} \right)$, where $i(j)$ runs from 1 to $n_{NN}(n_{SS})$, the number of observations when both spacecraft are north (NN) or both south (SS) of the current sheet. The first character of the two character identifier represents the magnetic field region for V1, the second for V2. Data for NS and SN configurations are also collected and are used independently, and in combination with the NN and SS data, to estimate G_r .

2. Data Selection.

This study covers the period from day 240, 1981 until day 190, 1983, while the V1-V2 separation increased from 1.9 to 4.7 AU in radial distance from the sun and from 10° to 21° in latitude. V1 traveled from 11 to 17 AU and from 6°N to 20°N. V1-V2 longitude separation was $\leq 16^\circ$. Daily samples of counting rates of protons with energies >75 MeV and a median energy ~ 1.1 GeV measured by the nearly identical High Energy Telescopes of the Voyager Cosmic Ray Subsystem [Stone et al., 1977], and Γ the ratio of V1 to V2 counting rate samples are plotted in Figure 2. Calendar days for the NN and SS data sets are highlighted in the upper panel by underscoring. We have compared measurements taken at both spacecraft on the same day under the assumptions that convective effects are unimportant on the average, consistent with long-interval average observations [Venkatesan et al, 1983], and that local variations in the cosmic ray intensity, after eliminating solar flare transient effects, are due to variations in the distance to the current sheet [Newkirk and Fisk, 1985].

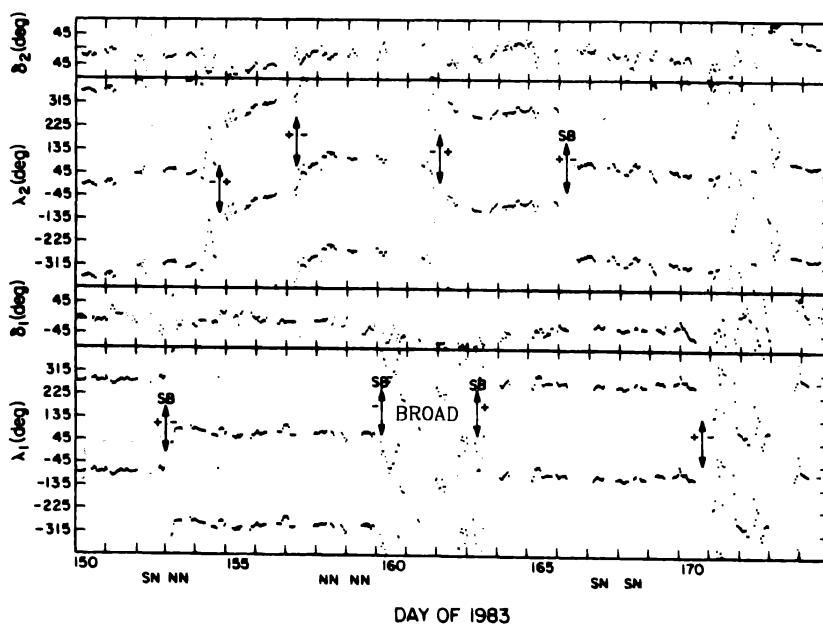
Fig. 2. Daily samples of the counting rates of >75 MeV protons from V1 and V2 (V1 is offset for clarity) and Γ the ratio of V1 to V2 counting rate samples. Uncertainties are due to counting statistics.



The counting rates of >75 MeV and ~ 1 MeV protons were used to eliminate periods possibly contaminated by solar flare particles and Forbush decreases. Proton energy spectra and elemental abundance measurements at lower energies were also used for this purpose. Hourly averages of the interplanetary magnetic field azimuth and elevation angles (Figure 3) measured by the Voyager Magnetic Field Experiment were used to determine the less active magnetic field periods, sector

polarities, and transition regions between sectors. Time blocks of data were identified when V1 and V2 were in regions of magnetic field pointing generally toward or away from the sun along the expected field direction, which is generally perpendicular to the radial direction in the outer solar system and parallel to the equatorial plane near the equator. The minimum sector length used herein is 4.5 days, so that V1 and V2 were most likely in field regions associated with plasma flows from the sun's polar coronal holes. This produced Data Set (DS) I. Then days with a poorly defined transition region at either end of the magnetic sector and days with azimuthal turbulence were eliminated in order to produce DS II. Finally, days with elevation angles pointing away from the equatorial region and days with elevation angle turbulence were collected into subset DS IIb. When the elevation angle changes by a large amount in less than a day or two as in DS IIb, it is likely to represent a dynamical effect such as the passage of transient material or perhaps reconnection at a sector boundary, either of which could alter the cosmic ray gradient. Those quietest days remaining are subset DS IIa.

Fig. 3. Magnetic field azimuth and elevation angles from V1 and V2. The azimuth, λ , is 0° when the field is directed away from the sun and the elevation, δ , is 0° when the field is along the spacecraft-sun line. Two cycles of λ are plotted. Arrows highlight transition regions interpreted as current sheet crossings. Those labeled "SB" are similar to sector boundaries at 1 AU.



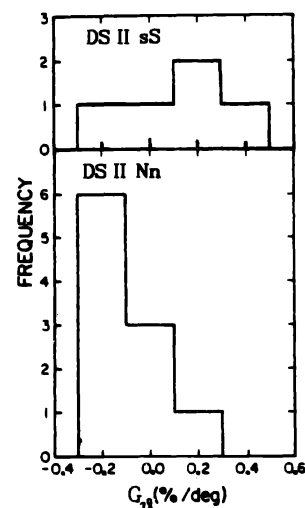
3. Observations and Discussion. Determination of $\langle G_\theta \rangle$ requires knowledge of the value of G_r , which can be estimated from NS and SN data sets, since the latitude gradients, which have opposite signs in the two hemispheres should average to zero. Averaged over NS and SN, $\langle G_r \rangle_{NSSN} = 2.21 \pm 0.11 \text{ \%/AU}$, consistent with radial gradients reported by [Venkatesan et al., 1983]. G_r can also be determined by averaging the NN and SS data sets, assuming that G_θ is negligible. This results in $\langle G_r \rangle_{NNSS} = 2.29 \pm 0.13 \text{ \%/AU}$, consistent with $\langle G_r \rangle_{NS,SN}$, and suggesting that the best estimate is the average over all 152 days of data which yields $\langle G_r \rangle = 2.25 \pm 0.08 \text{ \%/AU}$. Note that an uncertainty of 0.1 \%/AU in the assumed G_r introduces an error of only 0.01 \%/deg in the derived $\langle G_\theta \rangle$.

$\langle G_\theta \rangle$ and $\langle G_\phi \rangle$ have been calculated both without restrictions on spacecraft position (unrestricted average), and with restrictions on spacecraft position with respect to the current sheet based upon time to or from the closest sector boundary crossing (restricted average). Requiring V2 to be closer to the current sheet than V1 for NN data and V1 closer than V2 for SS data (see e.g., Figure 1), should enhance the measured $\langle G_\theta \rangle$.

Table 1. $\langle G_\theta \rangle$ and $\langle G_\phi \rangle$ (# : days of observation)

unrestricted average			
DS	$\langle G_\theta \rangle_{NN}$ (%/deg)	$\langle G_\theta \rangle_{sS}$ (%/deg)	$\langle G_\phi \rangle$ (%/deg)
I	0.02 ± 0.03 (52) [#]	-0.02 ± 0.04 (22)	0.02 ± 0.03 (74)
II	0.03 ± 0.04 (29)	-0.01 ± 0.04 (19)	0.02 ± 0.03 (48)
Ila	-0.02 ± 0.05 (21)	-0.06 ± 0.03 (6)	-0.01 ± 0.04 (27)
Ilb	0.14 ± 0.09 (8)	0.01 ± 0.05 (13)	0.06 ± 0.05 (21)
restricted average			
DS	$\langle G_\theta \rangle_{Nn}$ (%/deg)	$\langle G_\theta \rangle_{sS}$ (%/deg)	$\langle G_\phi \rangle$ (%/deg)
I	-0.12 ± 0.04 (21)	0.09 ± 0.07 (7)	-0.11 ± 0.03 (28)
II	-0.18 ± 0.05 (10)	0.12 ± 0.09 (5)	-0.16 ± 0.04 (15)
Ila	-0.18 ± 0.05 (10)	-0.06 ± 0.08 (1)	-0.15 ± 0.05 (11)
Ilb	----- (0)	0.20 ± 0.09 (4)	-0.20 ± 0.09 (4)

Table 1 lists values of $\langle G_\theta \rangle$ and $\langle G_\phi \rangle$ for both positional criteria (the lower case subscript is for the spacecraft closer to the current sheet) using $G_r = 2.25$ %/AU for the radial gradient correction. Note that the unrestricted $\langle G_\phi \rangle$ displays no observable gradient, while the restricted $\langle G_\phi \rangle$ is statistically significant and is approximately -0.15 ± 0.05 %/deg. Since differences between DS Ila and DS Ilb are statistically insignificant, we have no evidence that field elevation turbulence affected our measurements. Figure 4 shows the separation of the Nn and sS subsets for DS II with the restricted average. Note that, even with such a small data set, a separation of means and modes of the Nn and sS distributions, attributable to a small, negative latitude gradient, is evident. Further studies are required to determine whether such gradients are typical of other time periods.

Fig. 4. $\langle G_\phi \rangle$ for DS II, restricted average.

4. Acknowledgements. We are grateful for the contributions of R.E. Vogt, other Voyager Cosmic Ray Subsystem team members, and N.F. Ness. Work at Caltech was supported in part by the National Aeronautics and Space Administration under contract JPL 49-556-63120-0-2600 and grant NGR 05-002-160.

References

- Decker, R. B., S. M. Krimigis, and D. Venkatesan [1984], *Astrophys. J. Lett.*, **278**, L119.
 Hoeksema, J. T. [1984], *Ph.D. Thesis*, Stanford University, Stanford CA.
 Kota, J and J. R. Jokipii [1983], *Astrophys. J.*, **265**, 573.
 Newkirk, G., J. Lockwood, M. Garcia-Munoz, and J. A. Simpson [1984], *EOS, Trans, Am. Geophys. U.*, **65**, 1034.
 Newkirk, G. and L. A. Fisk [1985], *J. Geophys. Res.*, **90**, 3391.
 Venkatesan, D., Decker, R. B., and S. M. Krimigis [1984], *J. Geophys. Res.*, **89**, 3735.